Supporting Information

Oxygen Vacancy Modulated Homojunction Structural $CuBi_2O_4$ for Efficient Solar Water Reduction

Shenqi Wei,[a] Chenglong Wang,[a] Xuefeng Long,[a] Tong Wang,[a] Peng Wang,[a] Mingrui Zhang,[b] Shuwen Li,[a] Jiantai Ma,[a] Jun Jin*[a] and Lan Wu*[b]

[a]State Key Laboratory of Applied Organic Chemistry (SKLAOC), The Key Laboratory of Catalytic Engineering of Gansu Province College of Chemistry and Chemical Engineering, Lanzhou University Lanzhou, Gansu, 730000, P. R. China

E-mail: jinjun@lzu.edu.cn

[b]College of Chemical Engineering, Northwest University for Nationalities, Lanzhou, Gansu 730030, P.R. China

E-mail:wulan@xbmu.edu.cn

The equations

The conversion between potentials versus Ag/AgCl and versus RHE is determined using the equation below.

$$E(\text{versus RHE}) = E(\text{versus Ag/AgCl}) + E_{\text{Ag/AgCl}}(\text{refer}) + 0.0591\text{V} \times \text{pH}$$

$$E_{\text{Ag/AgCl}}(\text{refer}) = 0.197 \text{ V versus NHE at } 25\ ^{o}\text{C} \qquad (1)$$

Incident photon to current efficiency (IPCE) was obtained using an Oriel Cornerstone 260 1/4 m monochromator with a 500W Oriel Xe lamp as the simulated light source (LSH-X500B). An applied potential of 1.23 V vs. RHE was supplied by a miniature integrated electrochemical workstation (Zolix Instruments Co., Ltd). IPCE values were calculated using the equation below

$$IPCE(\%) = \frac{J \times 1240}{\lambda \times P_{light}} \times 100\% \qquad (2)$$

J refers to the photocurrent density (mA cm^{-2}) obtained from the electrochemical workstation. λ and P_{light} are the incident light wavelength (nm) and the power density obtained at a specific wavelength (mW cm^{-2}), respectively.

Applied bias photon-to-current efficiency (ABPE) can be calculated using the following equation:

$$ABPE(\%) = \frac{J \times (1.23 - V_b)}{P_{light}} \times 100\% \qquad (3)$$

J refers to the photocurrent density (mA cm^{-2}) obtained from the electrochemical workstation. V_b is the applied bias vs. RHE (V), and P_{light} is the total light intensity of AM 1.5 G (100 mW cm^{-2}).

The light absorption efficiency or light harvesting efficiencies (LHE, defined as the ratio of absorbed light to the incident light) of each photoanodes are calculated from their UV−Vis absorption spectra:

$$LHE = 1 - 10^{-A(\lambda)} \qquad (4)$$

where A(λ) is the absorbance at a specific wavelength. In order to calculate J_{abs} (the photocurrent density achievable assuming 100% absorbed photon–to–current conversion efficiency for photons) the solar spectral irradiance at AM 1.5G ($W \cdot m^{-2} \cdot nm^{-1}$, ASTM G173−03) is first converted to solar photocurrents vs. wavelength ($A \cdot m^{-2} \cdot nm^{-1}$) assuming 100% IPCE for photons. Then the solar photocurrents are multiplied by the LHE at each wavelength and adding these products up.

According to the M-S curves, charge carrier density (N_d) can be calculated using the following equation:

$$N_d = \frac{2}{e\varepsilon_0\varepsilon} \times \left[\frac{d\left[\frac{1}{C^2}\right]}{dV_S}\right]^{-1} \qquad (5)$$

The electronic charge (e) is 1.6×10^{-19} C, vacuum permittivity (ε_0) is 8.854×10^{-14} F m^{-1}, and relative permittivity (ε) is 80 for CBO. C (F cm^{-2}) is the space charge capacitance in the semiconductor (obtained from M-S curves), and V_s (V) is the applied potential for M-S curves.

the efficiency of charge transport in the bulk (η_{bulk}, relating to bulk charge separation) and surface charge transfer efficiency ($\eta_{surface}$, the yield of holes that are involved in water oxidation reaction after reaching the electrode/electrolyte interfaces) of the prepared photoanodes, can be calculated using the following equations:

$$\eta_{bulk} = \frac{J^{Na_2SO_3}}{J_{abs}} \quad (6)$$

$$\eta_{surface} = \frac{J^{H_2O}}{J^{Na_2SO_3}} \quad (7)$$

J_{abs} is the unity converted photocurrent density from the light absorption, while J^{H2O} and J^{Na2SO3} are the photocurrent densities obtained in 1 M KOH electrolyte and 1 M Na_2SO_3 (pH 9.5), respectively.

The formula for calculating transient decay time D is as follows:

$$D = (I_t - I_s)/(I_m - Is) \quad (8)$$

in which I_t is the current at time t, I_s is the stabilized current, and I_m is the current spike. The transient decay time can be defined as the time at which ln*D*=-1.

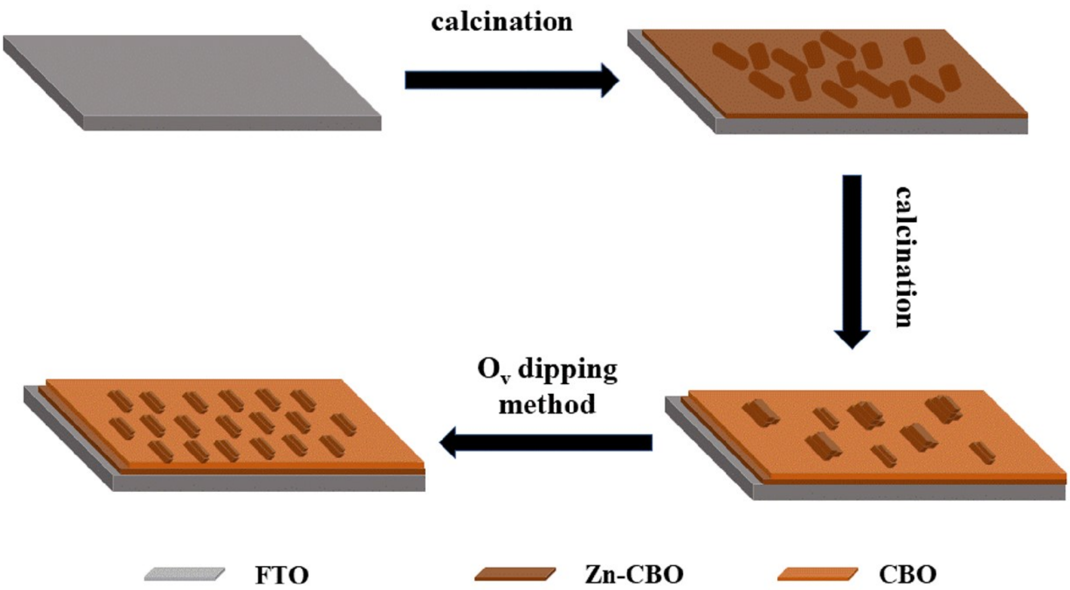

Scheme S1. Schematic diagram of the preparation procedure of the O_v/CBO/Zn-CBO photocathode.

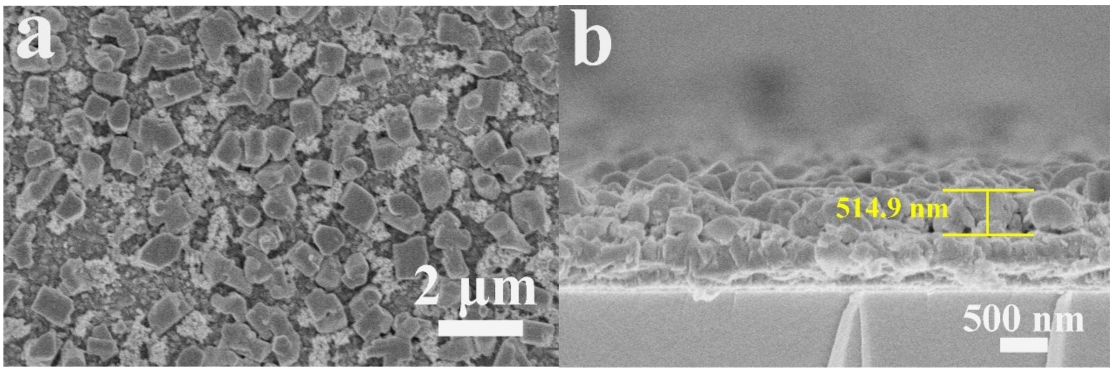

Figure. S1 Top-view SEM images of (a) CBO/Zn-CBO. Cross-sectional view SEM images of (b) CBO

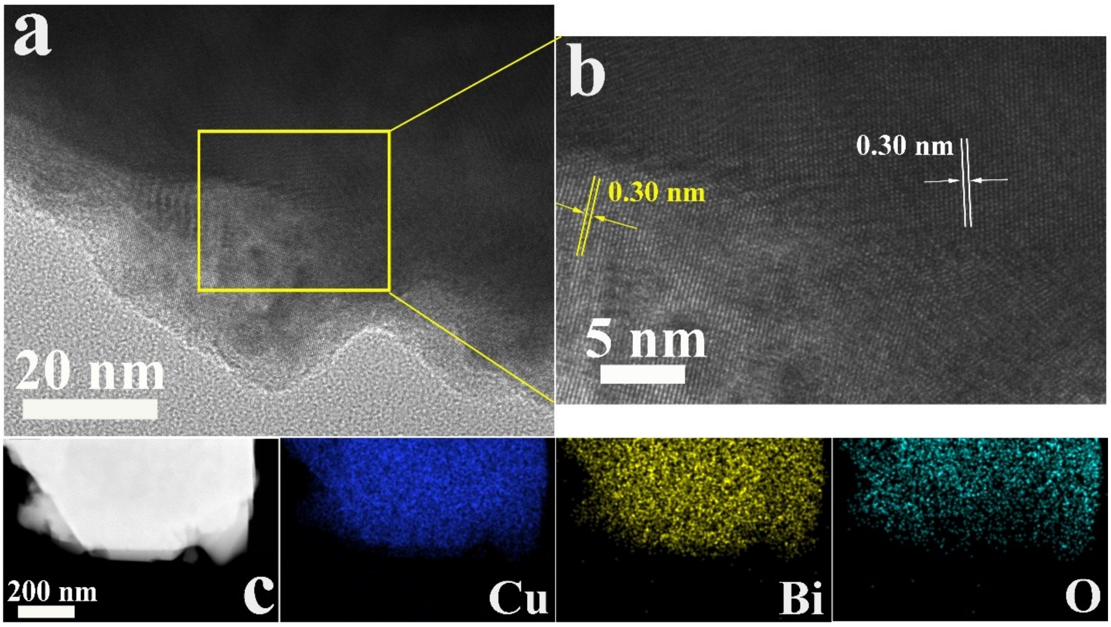

Figure. S2 TEM images of (a) CBO/Zn-CBO, HRTEM images of (b) CBO/Zn-CBO. (c) STEM-EDX element mapping for the CBO.

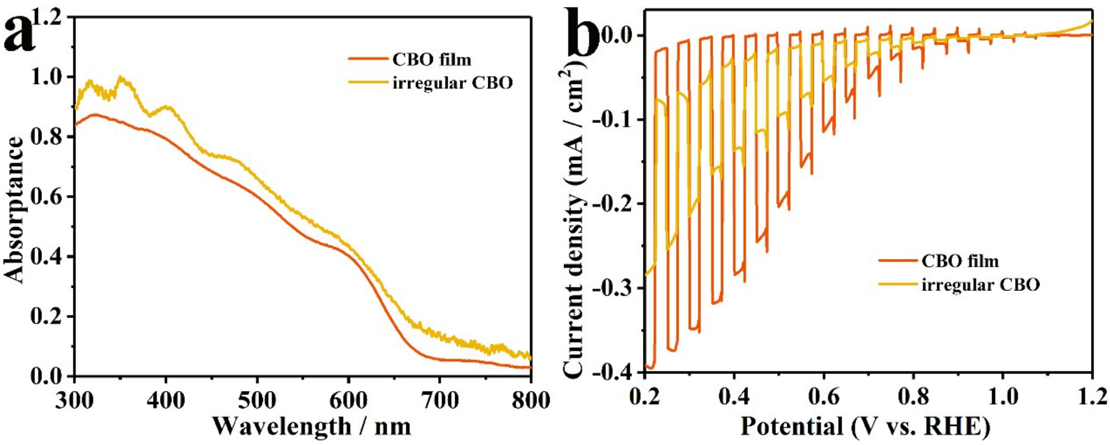

Figure. S3 (a) UV-visible diffuse reflection spectra and (b) Photocurrent density curves of CBO film and irregular CBO

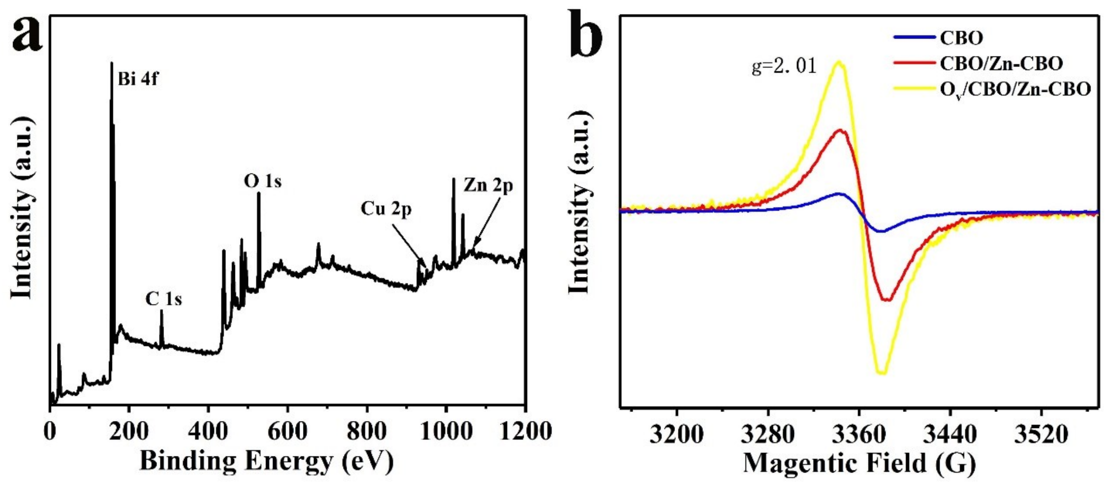

Figure S4. (a) XPS full spectrum (b) EPR measurements for CBO, CBO/Zn-CBO and O_V/CBO/Zn-CBO photocathodes.

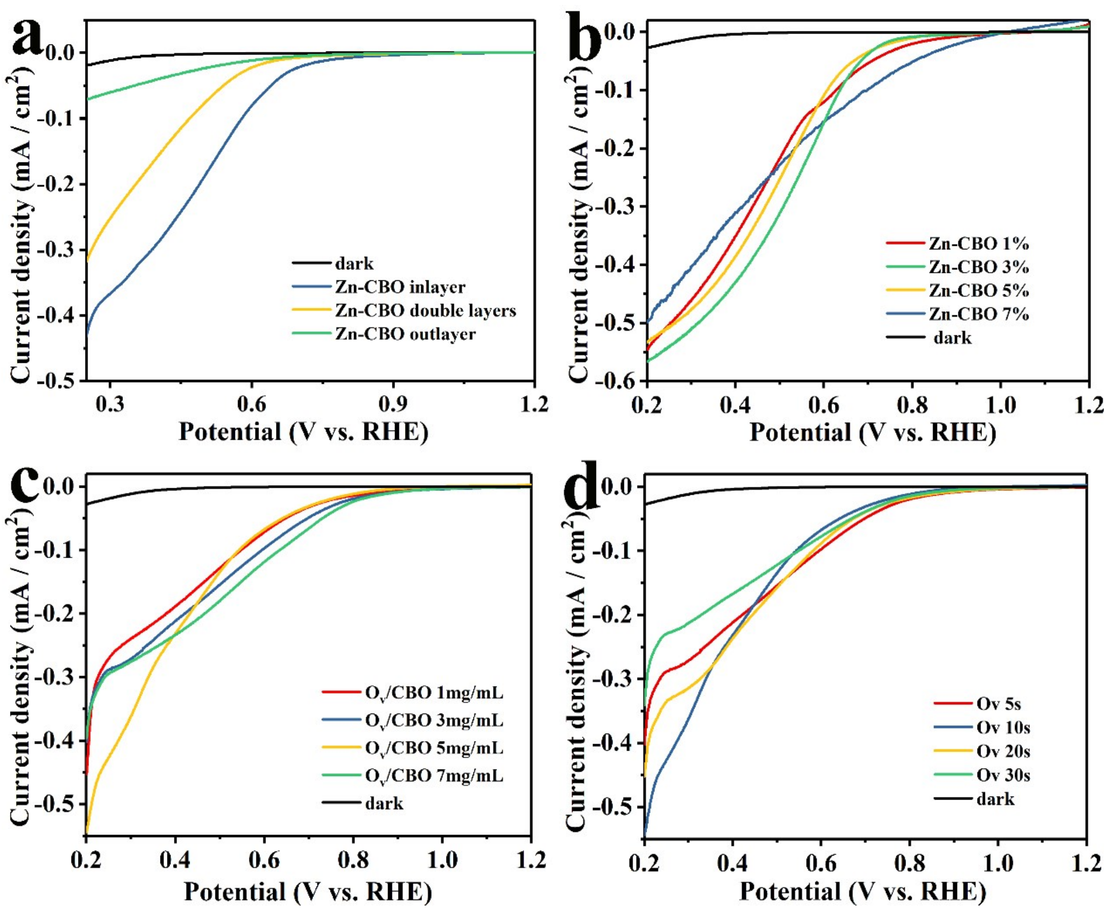

Figure S5. Photocurrent density curves of (a) Zn-doped CBO in different layers (inlayer out layer and double layers), (b) Zn-doped CBO at different concentrations (1 %, 3 %, 5 % and 7 %), (c) CBO treated with $NaBH_4$ of different concentrations (1 mg/mL, 3 mg/mL, 5 mg/mL and 7 mg/mL), (d) CBO dipping with $NaBH_4$ at different times (5 s, 10 s, 20 s and 30 s).

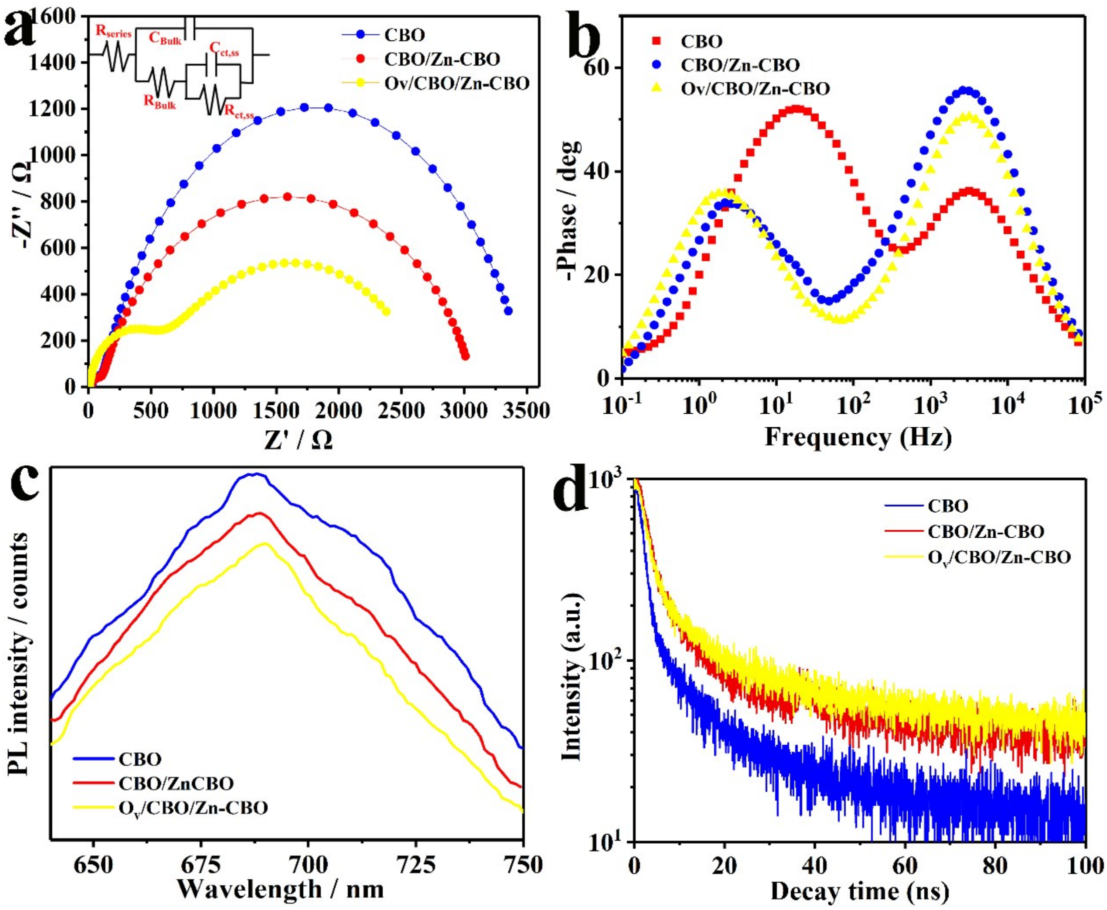

Figure S6. (a) Impedance curves (dark) and (b) Bode plots of the samples at 0.3 V vs. RHE under illumination (c) Steady-state photoluminescence emission spectra of all samples (d) photoluminescence decay curves of the samples.

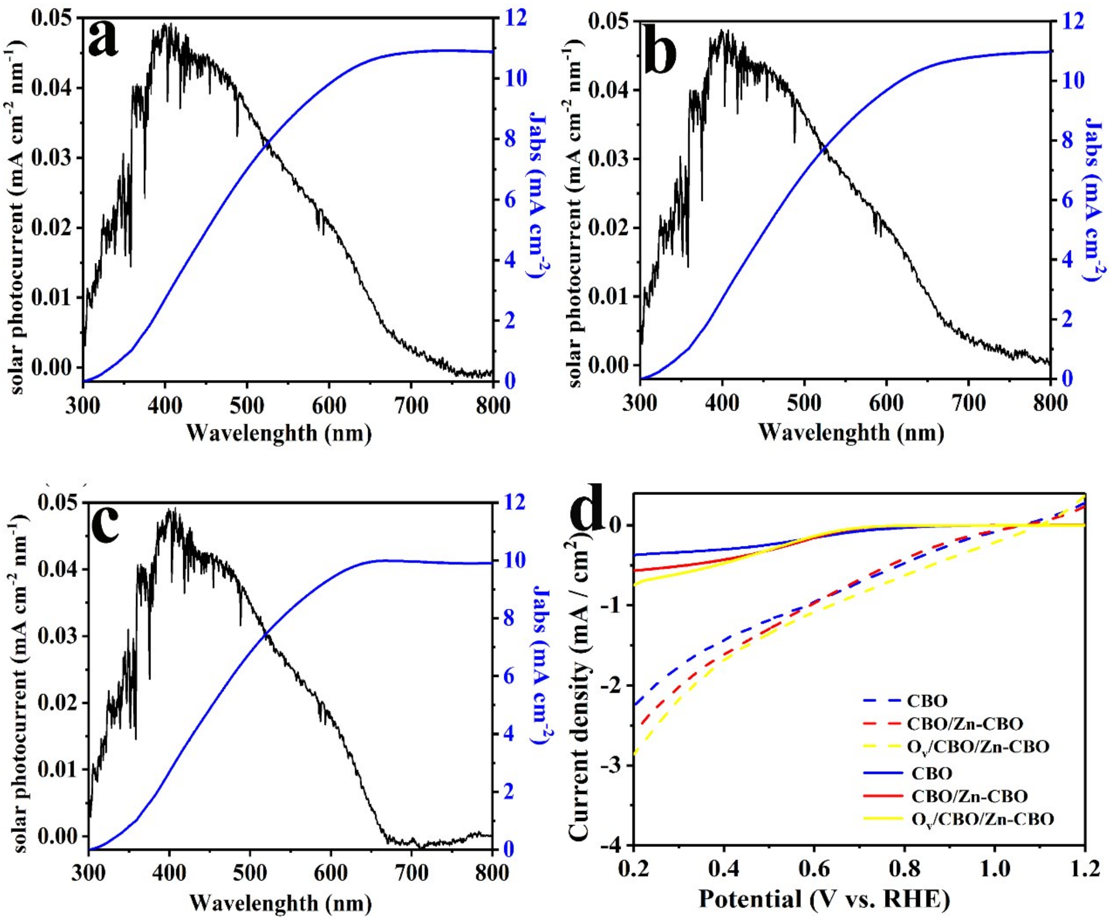

Figure S7. Jabs values of (a) CBO, (b) CBO/Zn-CBO, and (c) O_v/CBO/Zn-CBO photocathodes (assuming 100 % absorbed photon-to-current conversion efficiency for photons) (d) LSVs of CBO, CBO/Zn-CBO and O_v/CBO/Zn-CBO photocathodes with or without H_2O_2.

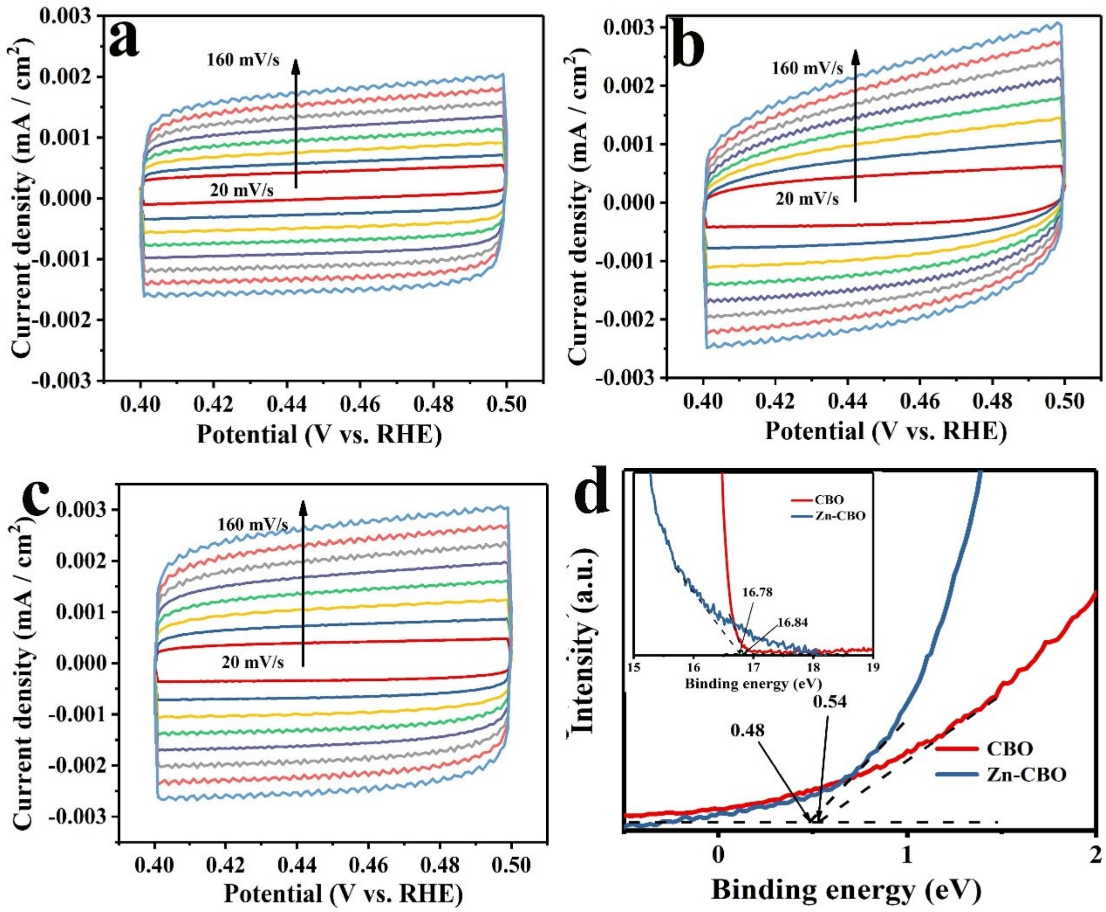

Figure S8. Voltammograms of the (a) CBO, (b) CBO/Zn-CBO, and (c) O_v/CBO/Zn-CBO photocathodes at various scan rates (20-160 mV/s) (d) UPS spectra for CBO and Zn-CBO photocathodes.

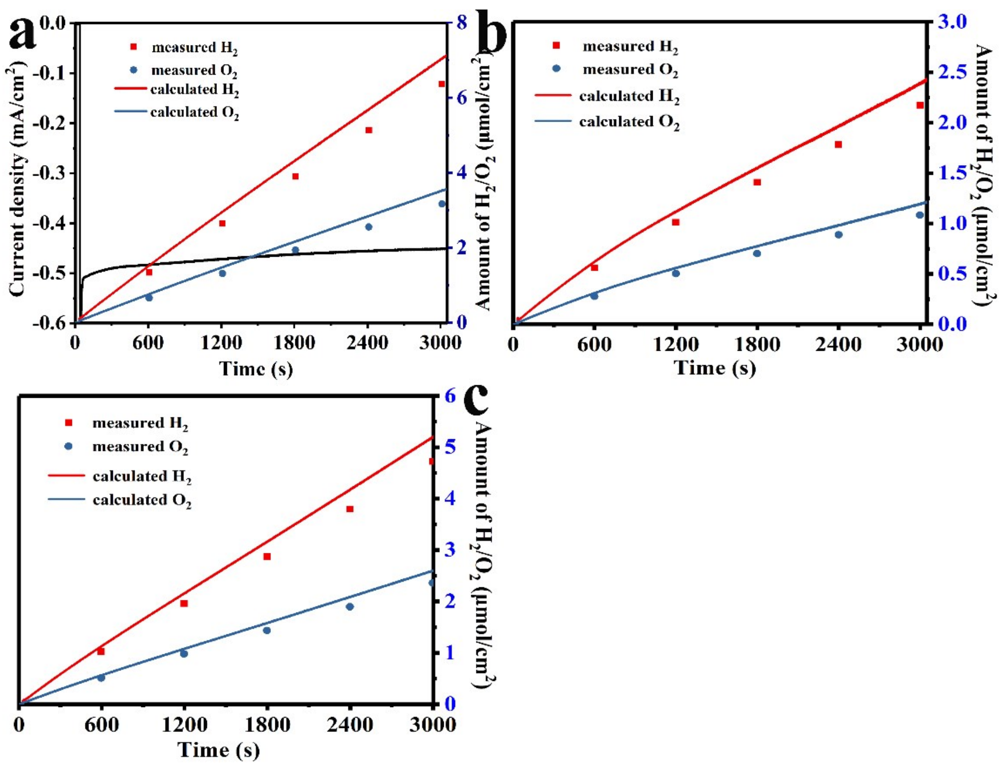

Figure S9 I–t curve and calculated (solid lines) and measured (dots) H_2 and O_2 evolution at 0.3 V vs. RHE over the (a) O_v/CBO/Zn-CBO (b) CBO and (c) CBO/Zn-CBO photocathode.

Table S1. Comparison of our photocathode to other $CuBi_2O_4$-based photocathode.

Year	Photocathode	Morphology	Electrolyte (pH)	Photocurrent density	Ref.
2020	$O_v/CuBi_2O_4$/Zn-$CuBi_2O_4$	irregular bumps	0.3 M K_2SO_4/0.2 M Phosphate buffer solution (pH 6.65)	0.6 mA/cm^2 at 0.3 V_{RHE}	This work
2014	$CuO/CuBi_2O_4$/Pt	film	0.3 M K_2SO_4, 0.1 M phosphate (pH 6.8)	0.71 mA/cm^2 at 0.4 V_{RHE}	Phys Chem Chem Phys, 2014, 16, 22462-22465
2014	$CuBi_2O_4$/CuO	nanoflower	0.1 M Na_2SO_4	0.38 mA/cm^2 at 0.3 V_{RHE}	J. Mater. Chem. A, 2014, 2, 3661-3668
2015	$CuBi_2O_4$	film	0.1 M Na_2SO_4 (pH 6)	0.01 mA/cm^2 at 0.3 V_{RHE}	J Mater Chem A, 2016, 4, 2936-2942
2016	$CuBi_2O_4$/ Ag-$CuBi_2O_4$	film	0.1 M NaOH (pH 12.8)	0.5 mA/cm^2 at 0.5 V_{RHE}	Chem Mater, 2016, 28, 4331-4340
2016	Au/$CuBi_2O_4$ /pt	film	0.1 M Na_2SO_4 (pH 6.8)	0.78 mA/cm^2 at 0.3 V_{RHE}	J Mater Chem A, 2016, 4, 8995-9001
2016	$CuBi_2O_4$ /pt	film	0.3 M K_2SO_4 and 0.2 M phosphate buffer (pH 6.65)	0.58 mA/cm^2 at 0.3 V_{RHE}	Chem Mater, 2016, 28, 4231-4242
2016	$CuBi_2O_4$	thin film	0.5 M Na_2SO_4 (pH 6)	0.105 mA/cm^2 at 0.3 V_{RHE}	Mater Lett, 2017, 188, 192-196.
2017	$CuO/CuBi_2O_4$ and α-$Bi_2O_3/CuBi_2O_4$	nanocomposite	0.1 M Na_2SO_4	0.23 mA/cm^2 ($CuO/CuBi_2O_4$) 0.05 mA/cm^2	J Phys Chem C, 2017, 121, 8252-8261
2017	$CuBi_2O_4$	thin film	0.3 M K_2SO_4 and 0.2 M phosphate buffer (pH 6.65)	Less than 0.3 mA/cm^2 at 0.6 V_{RHE}	J Mater Chem A, 2017, 5, 12838-12847
2017	$CuBi_2O_4$/PTh	porous film	0.3 M K_2SO_4 and 0.2 M NaPi (pH 6.66)	0.41 mA/cm^2 at 0.3 V_{RHE}	Int. J. Hydrogen. Energ. 2018 43 2064-2072
2018	$CuBi_2O_4$/Au/N, Cu-C	film	0.3 M K_2SO_4/0.2 M Phosphate buffer solution (pH 6.68)	0.31 mA/cm^2 at 0.5 V_{RHE}	ACS. Sustain. Chem. Eng. 2018 6 7257-7264.
2018	$CuBi_2O_4$	textured	0.1 M Na_2SO_4 aqueous solution (pH 6.8)	0.39 mA/cm^2 at 0.3 V_{RHE}	Chem Communs, 2018, 54, 3331-3334
2019	$CuBi_2O_4$/ZnSe/P25	film	0.3 M K_2SO_4/0.2 M Phosphate buffer solution (pH 6.65)	0.43 mA/cm^2 at 0.3 V_{RHE}	ChemElectroChem, 2019, 6, 3367-3374.
2019	Cu:NiO/$CuBi_2O_4$	film	0.3 M K_2SO_4/0.2 M Phosphate buffer solution (pH 6.65)	0.5 mA/cm^2 at 0.6 V_{RHE}	ChemElectroChem, 2019, 6, 3367-3374.
2020	$CuBi_2O_4$	Planar film	0.132 M KOH and 0.05 M KCl	0.68 mA/cm^2 at 0.25 V_{RHE}	J Mater Chem A, 2019, 7, 9183-9194
2020	$CuO/CuBi_2O_4$	film	0.5 M Na2SO4	0.9 mA/cm^2 at 0.1 V_{RHE}	Int J Hydrogen Energy, 2020, 45, 15121-15128.

1. H. S. Park, C. Y. Lee and E. Reisner, *Phys. Chem. Chem. Phys*, 2014, **16**, 22462-22465.
2. R. Patil, S. Kelkar, R. Naphade and S. Ogale, *J. Mater. Chem. A*, 2014, **2**, 3661-3668.
3. G. Sharma, Z. Zhao, P. Sarker, B. A. Nail, J. Wang, M. N. Huda and F. E. Osterloh, *J. Mater. Chem. A*, 2016, **4**, 2936-2942.
4. D. Kang, J. C. Hill, Y. Park and K.-S. Choi, *Chem. Mater*, 2016, **28**, 4331-4340.
5. D. Cao, N. Nasori, Z. Wang, Y. Mi, L. Wen, Y. Yang, S. Qu, Z. Wang and Y. Lei, *J. Mater. Chem. A*, 2016, **4**, 8995-9001.
6. S. P. Berglund, F. F. Abdi, P. Bogdanoff, A. Chemseddine, D. Friedrich and R. van de Krol, *Chem. Mater*, 2016, **28**, 4231-4242.
7. Y.-H. Choi, K. D. Yang, D.-H. Kim, K. T. Nam and S.-H. Hong, *Mater. Lett*, 2017, **188**, 192-196.
8. M. K. Hossain, G. F. Samu, K. Gandha, S. Santhanagopalan, J. P. Liu, C. Janáky and K. Rajeshwar, *J. Phys. Chem. C*, 2017, **121**, 8252-8261.
9. Q. Nie, L. Yang, C. Cao, Y. Zeng, G. Wang, C. Wang and S. Lin, *Chem. Eng. J*, 2017, **325**, 151-159.
10. N. Xu, F. Li, L. Gao, H. Hu, Y. Hu, X. Long, J. Ma and J. Jin, *Int. J. Hydrogen. Energy*, 2018, **43**, 2064-2072.
11. N. Xu, F. Li, L. Gao, H. Hu, Y. Hu, X. Long, J. Ma and J. Jin, *ACS. Sustain. Chem. Eng*, 2018, **6**, 7257-7264.
12. J. Li, M. Griep, Y. Choi and D. Chu, *Chem. Commun*, 2018, **54**, 3331-3334.
13. S. Wei, N. Xu, F. Li, X. Long, Y. Hu, L. Gao, C. Wang, S. Li, J. Ma and J. Jin, *ChemElectroChem*, 2019, **6**, 3367-3374.
14. A. Song, P. Plate, A. Chemseddine, F. Wang, F. F. Abdi, M. Wollgarten, R. van de Krol and S. P. Berglund, *J. Mater. Chem. A*, 2019, **7**, 9183-9194.
15. M. Li, X. Tian, X. Zou, X. Han, C. Du and B. Shan, *Int. J. Hydrogen. Energy*, 2020, **45**, 15121-15128.
16. S. Pulipaka, N. Boni, G. Ummethala and P. Meduri, *J. Catal*, 2020, **387**, 17-27.